Peter Adel (Autor)

Pulsed fiber Lasers

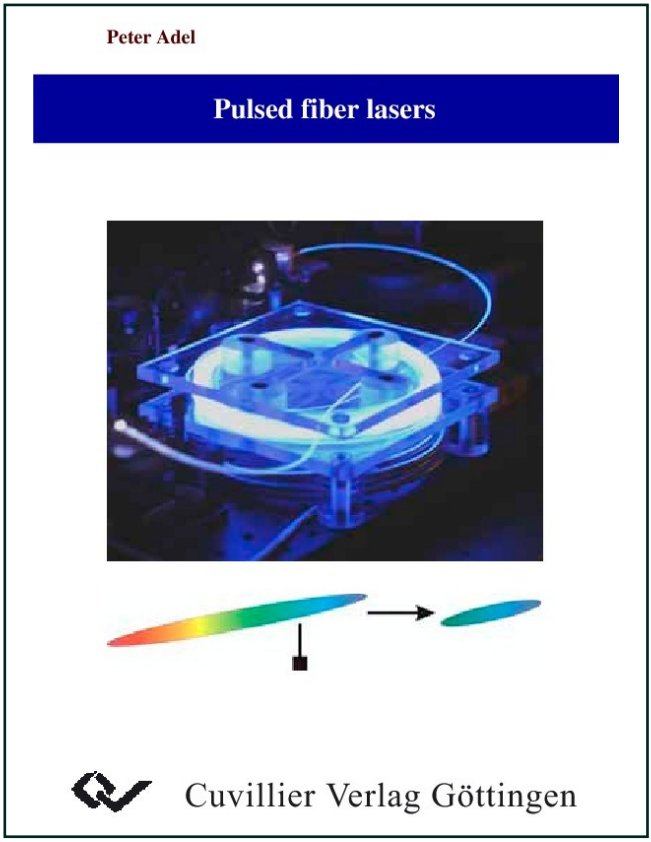

https://cuvillier.de/de/shop/publications/2908

1 Introduction

Continuous wave and pulsed solid-state lasers have revolutionized many areas like material processing, metrology, medicine, spectroscopy and basic scientific research. One prominent representative of these laser systems, the Ti:sapphire laser, is nowadays commercially available and has become the working horse for many applications. The versatility and the wide use of this laser is attributable to the large gain bandwidth of its laser material, which enables generation of ultrashort pulses as well as tunable laser operation over a broad wavelength range. Additionally, ultrashort pulses with energies of up to several millijoules have been demonstrated from Ti:sapphire based oscillator-amplifier systems. However, this laser material has also several drawbacks, as it must be pumped by gas lasers or frequency-doubled solid-state lasers. This results in a low overall efficiency, a large set-up and high system costs. Furthermore, the laser transition of Ti:sapphire has a lifetime of only about 3.2 microseconds and energy can be stored in this gain material only over a few microseconds. Thus, for repetition rates below several hundred kilohertz, pulsed Ti:sapphire lasers cannot be effectively pumped by continuous wave lasers. Moreover, the pulse repetition rate of oscillator-amplifier systems based on this gain material is usually limited far below 100 kHz, due to the required bulk electrooptic switches.

The broad gain bandwidth of rare-earth doped fibers, which is a result of the amorphous structure of silica glass, allows also tunable laser operation over a broad wavelength range and the generation of ultrashort pulses. However, compared to Ti:sapphire lasers, fiber based laser systems provide several advantages, as they can be efficiently pumped by laser diodes and can be realized in very compact set-ups. Additionally, the light guiding in the fiber results in a well-controlled beam shape, which is insensitive to thermal effects or external disturbances. Furthermore, energy can be stored in these fibers over a much longer time period, as the laser transitions have lifetimes of at least several hundred microseconds. Moreover, fiber-coupled electrooptic switches allow much higher repetition rates in fiber based oscillator-amplifier systems than for Ti:sapphire systems. Thus, potentially the output parameters of fiber based laser systems like wavelength, spectral width, pulse duration, pulse energy and repetition rate can be varied over a large range and adapted to the specific requirements of various applications. The objective of this work was therefore to develop fiber laser systems, which demonstrate the large variety of laser parameters that can be realized. For that reason,

three representative fiber laser set-ups were realized and investigating in detail during this work.

Generation of narrow linewidth laser pulses requires rather long pulse durations due to the Fourier limitation. Passive Q-switching is the preferred pulse generating mechanism for such laser systems, as it permits much longer pulses than mode-locking and it requires no additional control electronics. Commonly, saturable absorbers on the basis of Cr^{4+}-doped crystals or ceramics were used for initiating Q-switched laser operation in the near infrared. However, for fiber-based laser systems the use of such bulk elements results in a larger complexity and therefore the advantages of fiber-based systems cannot fully be exploited. Therefore, during this work a Q-switched fiber laser was developed, in which the saturable absorption was provided to the first time by a Thulium codoping in the gain fiber. By this way, the restrictions due to the previously required additional bulk saturable absorber can be overcome. The advantages of such a fiber-laser system can only be reached directly, if the various laser parameters can be adapted to the specific requirements. Thus, the Q-switching by the saturable absorption of the Thulium ions and the dynamics of the pulse generation were investigated experimentally and theoretically.

Much shorter pulse durations and larger spectral bandwidths can be generated by mode-locked lasers systems. However, most mode-locked fiber laser systems were directly pumped into the active fiber core. Therefore, these systems required high beam quality pump diodes, while the output power was rather limited. In combination with the cladding pumping scheme, fiber lasers can also be pumped by high power laser diodes with low beam quality. An important goal of this work was therefore the realization of a cladding pumped passive mode-locked Ytterbium-fiber laser.

Furthermore, spectral broadband laser sources with single mode-quality were needed for optical measurement techniques, like optical coherence tomography. This request is attributable to the fact, that the spectral bandwidth determines the minimum achievable resolution of such metrology systems. Therefore, an increase of the spectral bandwidth of mode-locked Ytterbium fiber lasers was a further goal of this work.

There is also a strong demand for compact and reliable high beam quality laser systems, which deliver pulse energies in the microjoule range at high repetition rates in combination with femtosecond pulse durations. This demand is driven by applications like fs-Lasik refractive surgery [HML03], writing of waveguides in silica glass [WNC02] [SBG01] or generation

of THz radiation [CLD02]. However, so far, the output pulse energies of femtosecond mode-locked fiber lasers are limited to several nanojoules. In order to overcome this limitation an oscillator-amplifier set-up was chosen, since such a set-up enables a scaling of the pulse energy to higher values, while the temporal pulse properties are still largely determined by the oscillator. Erbium fibers were chosen as gain material, since at the emission wavelength of these fibers at about 1.55 µm, the required fiber optic components are widely used for telecom applications and these components are reliable, relatively cheap and readily available. Furthermore, in combination with a nonlinear crystal, the output wavelength of such an oscillator-amplifier system matches the typical signal wavelength of conventional Ti:sapphire lasers. This strongly simplifies a replacement of Ti:sapphire lasers by this system.

The content of the work is arranged as follows: In chapter 2, the basic properties of pulsed fiber laser lasers are described. This description includes the various linear and nonlinear effects, which influence the pulse generation and propagation in the fibers, the properties of the used gain materials and the employed pulse generating mechanism. Chapter 3 focuses on the properties of a passively Q-switched Ytterbium fiber laser system. Based on the experimental results, the influences of the various physical effects on system operation are discussed. Chapter 4 covers the experimental results and the system properties of the realized mode-locked Ytterbium fiber laser. The extremely broadband operation of such a laser system, which can be achieved by intra-cavity spectral filtering, is then described in chapter 5. A chirped pulse oscillator-amplifier system is covered in chapter 6. The high output pulse energies of this system strongly favor nonlinear effects during signal amplification. Thus, the influences of the various nonlinear effects on system operation are analyzed. Furthermore, the resulting limitations are discussed and various methods to overcome these limitations are described in this chapter. Finally, in chapter 7 the results of this work are summarized.

2 Basics of pulsed fiber laser systems

2.1 Basics of fiber optics

In the geometrical model, wave guiding of optical fibers is due to total reflection of light rays at the boundaries of the dielectric core. Light is trapped as long as the incident angle, at the boundary between fiber core and surrounding cladding, meets the requirement for total reflection. Total reflection of light rays at this boundary can only occur if the light is incident from a denser to a less dense medium. Hence, light guiding in optical fibers requires that the refractive index of the core is higher than the surrounding cladding. This picture gives an intuitive understanding of light guiding in optical fibers. However, it takes not the wave properties of the light into account.

Each refractive index profile where a central part is surrounded with lower refractive index material can act as a waveguide. Since optical fibers have usually cylindrical symmetry, the following discussion is focused on waveguides with such symmetry. However it should be noted, that in general waveguides can also have other shapes or even have a one-dimensional structure (e.g. planar waveguides).

Optical waveguides can be made from various transparent materials like plastic, silica, fluoride or chalcogenide glasses [YEH89][GGZ98]. Nevertheless, silica glass is the material of choice for optical fibers in most cases. This is due to the extremely low optical loss, the good mechanical and chemical properties of this material and that it is non-toxic. The refractive index difference between the core and the cladding is realized during the fabrication process by adding dopants for increasing or decreasing the refractive index. Typically, germanium and phosphor are added for increasing the refractive index while boron and fluorine doping decrease it.

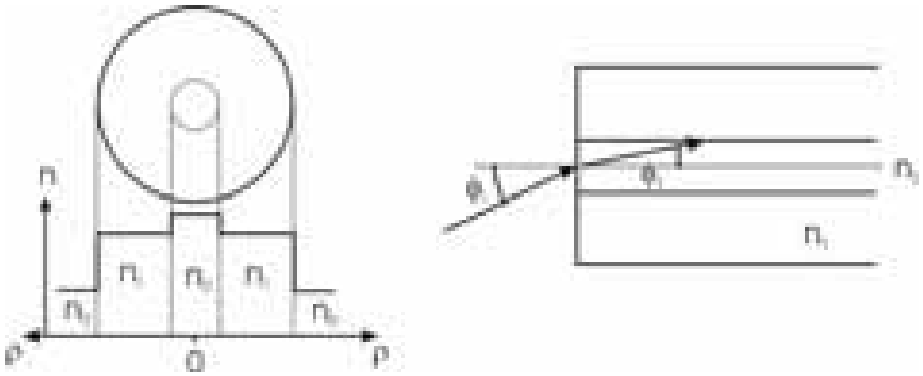

Fig. 2.1.1 *Left side: Index of refraction profile of a step-index fiber. n_0 is the index of the surrounding medium. Right side: Sketch for determining the numerical aperture of a step-index fiber.*

The simplest waveguide structure is a step in index profile, which has a constant refractive index in the core and in the cladding. Step index profiles are commonly used for optical fibers, since such structures are easier to manufacture than complicated index shapes. A schematic picture of the cross section and the refractive index profile of such a fiber is shown in figure 2.1.1. The refractive index difference between core and cladding determines the maximum incident angle θ_t at this boundary for total reflection. This boundary condition determines also the maximum acceptance angle of the fiber at the end facet, which is illustrated on the right side of figure 2.1.1. The sine of this angle is given by equation 2.1.1 and is called the numerical aperture NA of the fiber[1].

$$NA = n_0 \sin(\phi_i) = n_2 \sin(\phi_t) = \sqrt{n_2^2 - n_1^2} \tag{2.1.1}$$

2.1.1 Fiber modes

The previous geometrical approach is a good approximation if the core diameter of the fiber is several orders larger than the wavelength of the guided light. However, typically the wave properties of light must be taken into account, as these highly affects the signal propagation in a fiber. Based on Maxwell equations and the cylindrical symmetry of the fiber, it can be derived that the radial distribution of the transversal electric is determined in each sector by a differential equation for Bessel functions. The differential equations for the three cylindrical coordinates and the corresponding general solutions are shown in equations 2.1.2 – 2.1.6, where J_m, Y_m, K_m and I_m are different kinds of Bessel functions [AGR97]. The constant β in the solution of equation 2.3 shows the physical significance of a phase propagation constant.

$$d^2\Phi / d\phi^2 + m^2\Phi = 0 \tag{2.1.2}$$
$$\Rightarrow \quad \Phi = \exp(im\phi) \qquad m \in Z$$
$$d^2Z / dz^2 + \beta^2 Z = 0 \tag{2.1.3}$$
$$\Rightarrow \quad Z = \exp(i\beta z)$$
$$\frac{d^2F}{d\rho^2} + \frac{1}{\rho}\frac{dF}{d\rho} + \left(n^2 k_0^2 - \beta^2 - \frac{m^2}{\rho^2}\right) = 0 \tag{2.1.4}$$
$$\Rightarrow$$
$$F(\rho) = A\, J_m(\kappa\rho) + B\, Y_m(\kappa\rho) \qquad : \quad n \geq \beta / k_0 \tag{2.1.5}$$
$$\kappa^2 = n^2 k_0^2 - \beta_2$$
$$F(\rho) = C\, K_m(\gamma\rho) + D\, I_m(\gamma\rho) \qquad : \quad n < \beta / k_0 \tag{2.1.6}$$
$$\gamma^2 = \beta_2 - n^2 k_0^2$$

[1] The numerical aperture of a fiber is usually defined according to equation 2.1.1, although it is not very accurate for single-mode fibers. A more accurate description takes into account, that the output is essentially Gaussian in behavior and that the mode field diameter (MFD) in the fiber defines the beam waist for the output beam. Defining the MFD by the 1/e² intensity drop it can be shown that the NA is defined by $NA_{eff} = 2\lambda/(\pi\, MFD)$.

It can be also derived from Maxwell equations, that the tangential electric field and its first derivative must be continuous at the refractive index boundaries of an optical fiber [GUE90]. Furthermore, the field must be finite in the center and for a guided modes it must additionally decay roughly exponential for large ρ. It can be easily derived from the later of these conditions that for a step index fiber the constants B and D must be zero. The boundary condition at the index step results in an eigenvalue equation for the propagation constant β. Each eigenvalue β uniquely determines a field distribution and the corresponding fiber mode. Based on the constant β, an effective index n_{eff} can be defined for each mode (eqs. 2.1.7). This effective or mode index determines the propagation of a mode.

$$n_{eff} = \beta / k_0 = \beta \lambda / 2\pi \tag{2.1.7}$$

In general, the eigenvalue equation for β may have several solutions for each integer value of m. The number of the eigenvalues of β or the fiber modes depends on signal wavelength and the index profile of the fiber. For step index fibers, the two relevant design parameters are the numerical aperture NA and the core radius a. Usually, this relation is described by the normalized frequency V (eqs. 2.1.8).

$$V = k_0 \cdot a \cdot \sqrt{n_2^2 - n_1^2} = k_0 \cdot a \cdot NA \tag{2.1.8}$$

For large V values, a rough estimate for the number of the supported fiber modes is given by $V^2/2$, while for V-values below 2.405 only the fundamental mode is supported [AGR95]. The value of 2.405 is determined by the above mentioned eigenvalue equation and corresponds to the smallest solution for $J_0(V) = 0$. The cut-off wavelength of a fiber can be calculated by setting V = 2.405 and using $k_0 = 2\pi/\lambda$. For wavelengths below this cut-off, a fiber supports several modes and is therefore multi mode (MM) while it is single mode (SM) for longer wavelengths.

For the fundamental mode m = 0 and the field distribution has no zero except for $\rho \rightarrow \infty$. In addition, in a multi-mode fiber this mode has the highest eigenvalue β. The field distribution for this mode is described by the equations 2.1.9 and 2.1.10, where the constant A is determined by the signal power. For arbitrary refractive index profiles the numerical calculation of the propagation constant β and the corresponding field distribution is described in Appendix A.

$$F(\rho) = A\, J_0(\kappa \rho) \qquad \rho \le a \tag{2.1.9}$$

$$F(\rho) = \frac{A\, J_0(\kappa a)}{K_0(\gamma a)} K_0(\gamma \rho) \qquad \rho \ge a \tag{2.1.10}$$